Rapid degradation of alkanethiol-based self-assembled monolayers on gold in ambient laboratory conditions

Trevor M. Willey [a,b,*], Andrew L. Vance [a], T. van Buuren [a], C. Bostedt [a,1], L.J. Terminello [a], C.S. Fadley [b,c]

[a] *Lawrence Livermore National Laboratory, 7000 East Avenue, Livermore, CA 94550, USA*
[b] *University of California, Davis, CA 95616, USA*
[c] *Lawrence Berkeley National Laboratory, Berkeley, CA 94720, USA*

Abstract

Self-assembled monolayers (SAMs) consisting of alkanethiols and similar sulfur-containing molecules on noble metal substrates are extensively used and explored for various chemical and biological surface-functionalization in the scientific community. SAMs consisting of thiol- or disulfide-containing molecules adsorbed on gold are commonly used due to their ease of preparation and stability. However, the gold–thiolate bond is easily and rapidly oxidized under ambient conditions, adversely affecting SAM quality and structure. Here, the oxidation of dodecanethiol on gold is explored for various 12-h exposures to ambient laboratory air and light. SAM samples are freshly prepared, air-exposed, and stored in small, capped vials. X-ray photoelectron spectroscopy (XPS) reveals nearly complete oxidation of the thiolate in air-exposed samples, and a decrease in carbon signal on the surface. Near-edge X-ray absorption fine structure spectroscopy (NEXAFS) at the carbon K-edge shows a loss of upright orientational order upon air exposure. Alternatively, the oxidation of the thiolate is minor when SAMs are stored in limited-air-containing small 15 ml vials. Thus, care must be taken to avoid SAM degradation by ensuring alkanethiolates on gold have sufficient durability for each intended environment and application.
© 2005 Elsevier B.V. All rights reserved.

---

* Corresponding author. Tel.: +1 925 424 6084; fax: +1 925 422 4665.
  E-mail address: willey1@llnl.gov (T.M. Willey).
[1] Present address: Technische Universität Berlin, Germany.

1. Introduction

Solution exposure of alkanethiols to gold creates easily formed, relatively stable self-assembled monolayers that can be used for chemically or biologically functionalizing surfaces. The stability of such monolayers to ambient conditions is often taken for granted; however, recent reports have cast the assertions into doubt by suggesting a limited shelf-life for alkanethiols on gold under e.g. biological conditions [1]. This paper first reviews some of the literature on degradation of SAMs under different types of exposure, then presents additional data on alkanethiols exposed to air, and discusses this important aspect in preparing functionalized surfaces.

Early laser desorption experiments first saw oxidation features in hexadecanethiol on gold exposed to air [2] but did not quantitatively explore the stoichiometry and assumed (possibly incorrectly) that the oxidation was small. Other mass spectrometry desorption studies found $-SO_2^-$ (sulfinate) and $-SO_3^-$ (sulfonate) species at the ends of oxidized molecular fragments [3,4].

Later, a method for SAM removal using ultraviolet light and the associated ozone (O_3) produced was reported [5], with the ozone allegedly oxidizing the thiolates. Subsequently, photochemical removal methods using wavelengths insufficient to create O_3 from O_2 degraded and removed an oxygen-containing mercaptoundecanoic SAM, but were slow in removing an alkanethiol [6]. These studies concluded that UV light and the presence of oxygen could remove SAMs from gold surfaces. Further exploration supports ozone as a primary culprit for SAM degradation. In one study, SAMs were exposed to N_2, pure O_2, H_2O and O_2, enclosed pressurized air, and O_3. Only the O_3 exposed thiolates oxidized [7]. Another showed that the presence of light was not required to oxidize the SAMs, and that highly-crystalline, Au(1 1 1) substrates fare better than rougher surfaces, but in both cases, sulfur moieties oxidized to both sulfinate and sulfonate [8]. Additional reports conclude that for alkanethiols, oxidation occurs extremely rapidly and efficiently through ozone exposure [7,9–11].

Morphological changes have also been reported for degrading alkanethiols. Scanning tunneling microscopy measurements found thiolates oxidize first at domain boundaries. The oxidized molecules begin forming a striped phase [2] [12] between pristine domains. A final "fluid" phase is both disordered and deforms the underlying gold surface [13].

The rapid degradation of sulfur–gold bonding must be understood for the utilization of SAMs, and even more importantly for use of more dilute surface-attached species such as catenanes or rotaxanes with a more exposed Au–S interface [14–17]. Here, we investigate the degradation of alkanethiols on substrates under ambient, atmospheric, laboratory conditions using X-ray photoelectron spectroscopy (XPS) and X-ray absorption spectroscopy (XAS). For simple SAMs, the changes in the sulfur, carbon, and oxygen chemistry and stoichiometry using XPS are quantitatively explored for five dodecanethiol-on-gold samples: (1) a freshly prepared sample, (2) a sample stored in capped vials in darkness, (3) a vial-stored sample under fluorescent lighting, (4) a sample simply exposed to air in the dark, and (5) a sample exposed to air in the light. XAS measurements were also carried out to investigate chemical and morphological changes on two samples: a fresh one, similar to sample (1) above, and a second exposed to ambient lighting and atmosphere overnight, in similar fashion to sample (5).

Compared to pristine films, SAMs oxidize readily when exposed to air, while oxidation is minor if the SAMs are stored in closed, air-containing vials. As the film oxidizes, the SAMs lose their ordered, orientationally upright nature.

2. Experimental

2.1. Reagents and materials

Reagents were purchased from commercial sources and used as received. Dodecanethiol (98%) was purchased from Aldrich. Ethanol (200

---

[2] Striped phases often appear during the formation (or in this case degradation) of self-assembled monolayers. They consist of molecules prostrate on the surface self-organized into parallel rows. They appear as "stripes" in STM measurements as seen in the two other references listed in this paragraph.

proof, USP, glass container) was purchased from Aaper and used as received. Fischer vials of 15 ml in volume with polyethylene stoppers were used for sample storage/aging. Au(1 1 1) substrates were formed by evaporating 5 nm Ti and then 100 nm Au on Si(1 0 0) under high vacuum. All gold substrates were hydrogen flame annealed immediately before use. [3]

2.2. Sample preparation

Samples were prepared by immersing freshly annealed gold substrates in 1 mmol dodecanethiol in ethanol for 24–36 h. Samples were pulled from solution, rinsed with ethanol, and blown dry with nitrogen. Samples for XPS measurements were as follows: the first sample was immediately introduced into ultra-high vacuum and subsequently analyzed. Other samples were placed in clean 15 ml vials. The second was placed in an air-containing stoppered vial, wrapped thoroughly in aluminum foil, and labeled "vial/dark". Sample 3 was placed in a capped vial and placed on the laboratory bench under common fluorescent lighting conditions and labeled "vial/light". The fourth vial was left open, but wrapped in foil and placed under a foil tent to allow some ambient air flow/exchange and labeled "air/dark". The final, fifth sample was placed in an open vial, placed on the bench under light and labeled "air/light". These samples were left overnight in the laboratory, and placed in UHV the next morning for analysis. For separate XAS measurements, two pristine SAMs were prepared in the same manner. The "fresh" sample was analyzed immediately, while the second was allowed to sit in the ambient laboratory conditions overnight.

2.3. Instrumentation

X-ray photoelectron spectra were recorded using a PHI Quantum 2000 XPS system. This apparatus uses a highly focused Al Kα monochromatic X-ray (1486.7 eV) source, and a hemispher-

ical electron energy analyzer. For these experiments, the analyzer pass energy was set to 23.5 eV while the X-ray source was set to 40 W and a 200 μm focal spot, giving an overall resolution of about 0.3 eV. Spectra were acquired at $\sim 10^{-9}$ Torr. Spectra were calibrated by setting the center of the strong Au $4f_{7/2}$ peak to 84.01 eV. Sulfur XPS spectral fits contain S 2p spin-orbit split components: S $2p_{3/2}$ (S $2p_{1/2}$), with branching ratio 2:1 and energy difference of 1.2 eV. Peaks were fit with pure Gaussian functions with error function (integrated Gaussian) backgrounds centered at the peak positions. Four doublets were allowed in the fits. Full width half maxima were allowed to vary between 0.8 eV and 1.3 eV.

X-ray absorption spectra were recorded at VUV BL 8.2 of The Stanford Synchrotron Radiation Laboratory (SSRL, SPEAR II) at the Stanford Linear Accelerator Center [18]. This beamline uses bend magnet radiation and a spherical grating monochromator. XAS experiments were conducted with an energy resolution of about 0.2 eV at the carbon K-edge and the sulfur L-edge. Absorption spectra were recorded using total electron yield (TEY) and were normalized to the incident beam via the current from a clean transmissive grid with a freshly evaporated gold coating. Spectra were recorded at a base pressure of less than 1×10^{-9} Torr. Orientational information was obtained using polarization-dependent NEXAFS features in spectra acquired at different X-ray beam incidence angles (θ_i and θ_j) through the ratio method in Eqs. (1) and (2) [19–21]

$$\frac{I_v(\Theta_i, A)}{I_v(\Theta_j, A)} = \frac{P(3A-1)\Theta_i - A + 1}{P(3A-1)\Theta_j - A + 1} \quad (1)$$

and

$$\frac{I_p(\Theta_i, \Gamma)}{I_p(\Theta_j, \Gamma)} = \frac{P(3\Gamma-1)\Theta_i - \Gamma - 1}{P(3\Gamma-1)\Theta_j - \Gamma - 1} \quad (2)$$

These two equations are for orbitals which can be modeled as collinear (intensities I_v) or coplanar (intensities I_p), respectively. In order to greatly simplify analysis, the intensities are left as functions of cosine squared, with $\Theta_i = \cos^2\theta_i$, $A = \cos^2\alpha$, and $\Gamma = \cos^2\gamma$, where θ is the angle between the sample and the incident radiation, α is the polar angle of the vector-like orbitals, γ is the

---

angle between the normal to the orbital-containing plane and sample normal. The polarization P, measured using the variation in intensity of the π^* feature in highly pyrolytic ordered graphite (HOPG) as a function of angle, was 88% in the horizontal plane.

3. Results

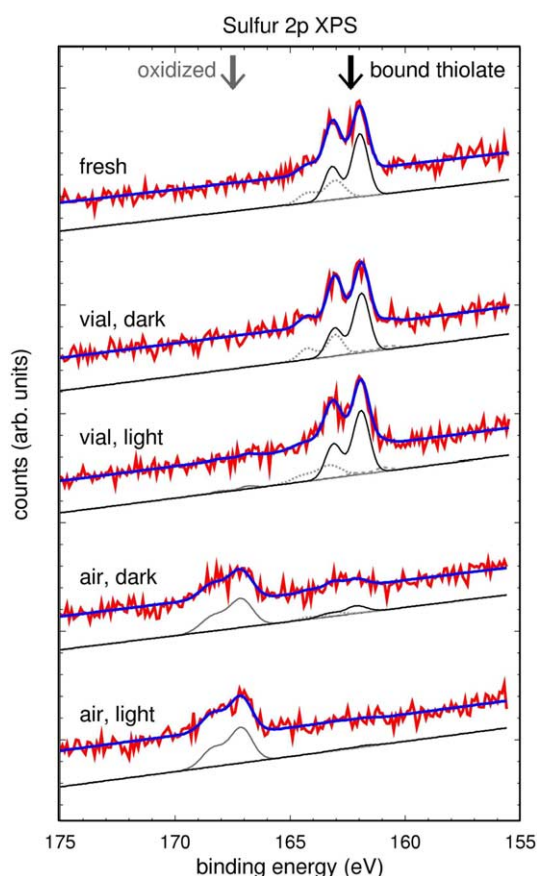Sulfur 2p XPS spectra are presented in Fig. 1. Spectra are presented from top to bottom for (1)

Fig. 1. Sulfur 2p XPS using an Al Kα source for dodecanethiol adsorbed on Au(111). For each specimen (see text for descriptions), the best fit is superimposed on the data while individual spin-orbit split components appear offset slightly for clarity. Primary components are bound thiolate and oxidized species indicated with arrows, while some unbound thiol and small amounts of elemental sulfur also appear and are indicated with dashed lines.

the freshly prepared SAM, (2) the sample in a capped vial stored in the dark, (3) the capped vial in the light, (4) the uncapped air-exposed sample in darkness, and (5) uncapped in the light. Presented in Fig. 1 are both data and best fit line for clarity. Four doublets were allowed in the fits, each corresponding to a particular sulfur species. These doublets are presented just below each data/best fit trace. Drastic changes occur in the sulfur spectrum. The fresh sample contains primarily a spin-orbit split doublet with S $2p_{3/2}$ at 161.97 eV. This feature vanishes in air-exposed samples, while a doublet at 167.09 eV appears. The peaks in this doublet also have a higher FWHM at around 1.2 eV rather than 0.85 eV. Fit component intensities are summarized in Table 1.

Sulfur X-ray absorption spectra are presented in Fig. 2 for a fresh dodecanethiol sample and one exposed to ambient laboratory conditions. Changes also occur in these spectra, with two prominent peaks appearing above the absorption onset at about 175 eV and 184 eV. Pre-edge features in the fresh sample at about 167 eV are also reduced in the air-exposed sample.

Oxygen 1s XPS spectra are presented in Fig. 3 for the same series of five preparation conditions. Oxygen concentrations are below detection limits for the fresh and vial-stored samples, as expected. However, for the air-exposed samples, the appearance of oxygen strongly supports oxidation of thiolate as shown in sulfur species previously presented in Fig. 1.

Carbon 1s spectra are presented in Fig. 4 for the series of samples. The integrated carbon signal is, as a percentage of the fresh SAM carbon intensity, 98% for the vial/dark, 97% for the vial/light, 68% for the air/dark, and 59% for the air/light. The peak position changes little for the vial-stored samples, but the air-exposed C 1s peaks are shifted to lower binding energy by about 0.75 eV. These air-exposed sample peaks are also broader, more asymmetric, and less intense. Carbon near-edge X-ray absorption fine structure (NEXAFS) spectra further investigate both chemical nature and orientation of molecules [20,21]. Spectra for the freshly prepared dodecanethiol-based SAM are presented in Fig. 5. Features include the sharp C–H σ^*/R* features near the absorption edge at

Table 1
S 2p integrated relative intensities, pristine/air-exposed SAMs

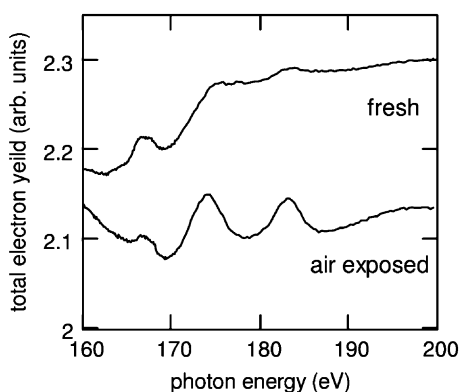| Monochrom. Al Kα S $2p_{3/2}$ (S $2p_{1/2}$) in eV	Elemental 160.91 (162.12)	Bound thiolate 161.97 (163.17)	Unbound/damaged 163.17 (164.36)	Oxidized 167.09 (168.30)
Fresh	–	74 ± 4%	26 ± 3%	–
Vial, dark	4 ± 4%	70 ± 4%	26 ± 4%	–
Vial, light	4 ± 4%	73 ± 4%	20 ± 4%	3 ± 3%
Air, dark	–	17 ± 7%	7 ± 7%	76 ± 6%
Air, light	–	3 ± 8%	–	97 ± 7%
Synchrotron, hv = 280 eV S $2p_{3/2}$ (S $2p_{1/2}$) in eV		161.9 (163.1)	163.4 (164.6)	166.8 (168.0)
Fresh	–	83 ± 5%	10 ± 4%	7 ± 5%
Air, light	–	43 ± 5%	8 ± 4%	49 ± 4%

Fig. 2. Sulfur L-edge XAS for dodecanethiol adsorbed on Au(111) fresh sample (top) and another left on the bench overnight uncovered (bottom).

Fig. 3. Oxygen 1s XPS for dodecanethiol adsorbed on Au(111): a strong O 1s peak appears in air-exposed samples.

around 288 eV, as well as the C–C σ* and C–C′ σ* features at roughly 293 eV and 301 eV respectively [22,23,20]. Spectra show a strong linear dichroism indicating a high degree of upright orientational order in the self-assembled monolayer. Analysis using Eq. (2) for the C–H σ*/R* features and Eq. (1) for σ* resonances indicate alkyl chains tilted 37 ± 7° from normal.

Carbon NEXAFS spectra for the sample exposed to air, however, show different behavior than the freshly prepared SAM. In Fig. 6, the air-exposed SAM, the spectra continue to have a small amount of dichroism, but much less than the fresh sample. Also, the first R*/C–H σ* feature is attenuated, but other σ* features look similar to the freshly prepared sample.
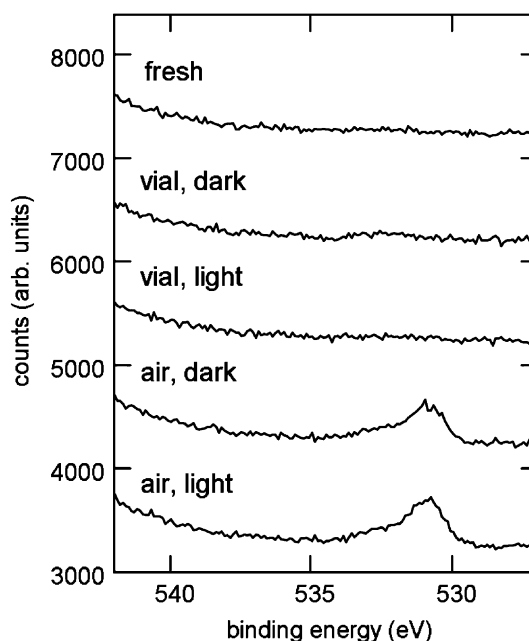
4. Discussion

The freshly prepared samples look as expected in sulfur 2p, carbon 1s, and oxygen 1s Al Kα XPS spectra. The main doublet S $2p_{3/2}$ peak at 161.97 eV is gold-bound thiolate [24], indicating monolayers well-bound to the substrate. The S 2p feature at 163.17 eV is consistent with sulfur species attributed to damage from the ionizing
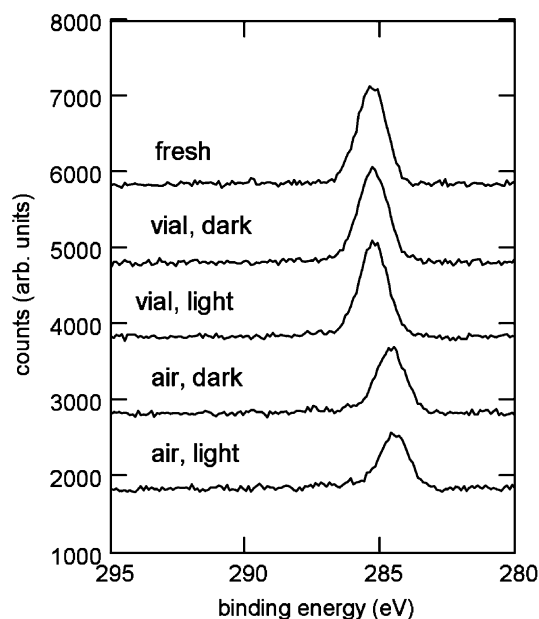
Fig. 4. Carbon 1s XPS for dodecanethiol adsorbed on gold: the C 1s peak is shifted, broadened, and less intense for air-exposed samples.

Fig. 6. Carbon NEXAFS for the sample exposed to air. Top: spectra acquired at normal (90°) and grazing incidence (20°); bottom: difference spectra.
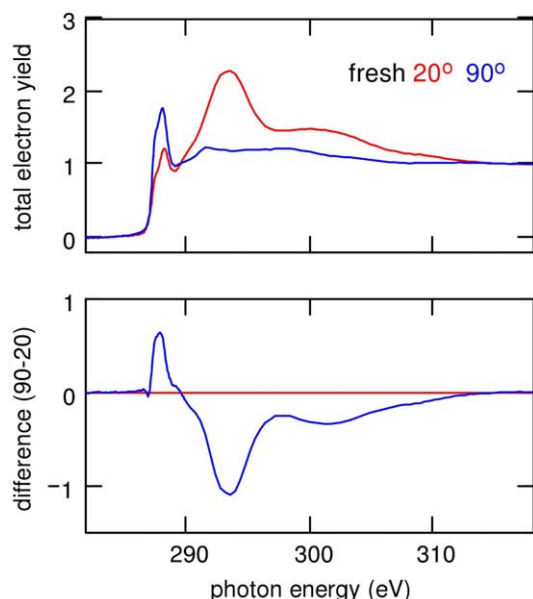

Fig. 5. Carbon NEXAFS for the freshly prepared and analyzed sample. Top: spectra acquired at normal (90°) and grazing incidence (20°); bottom: difference spectra.
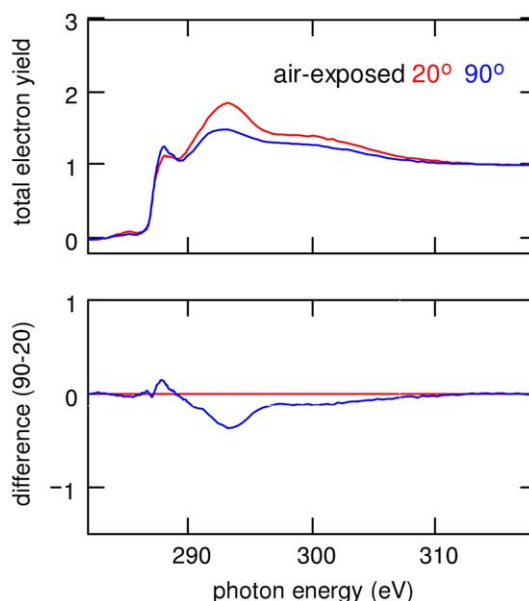
radiation [25–27], and is lower in binding energy than thiol [24]. This is quite plausible considering the long acquisition times and small focus (200 μm) of the X-rays in our laboratory source. Fresh samples exhibit carbon NEXAFS dichroism which returns the characteristic alkanethiol-on-gold tilt angle of well-ordered SAMs [28].

The SAMs stored in capped vials showed small changes. Sulfur and carbon compositions were similar, but a small decrease in carbon intensity and an increase in Au 4f intensity may indicate slight desorption of SAM molecules. Exposure to UV and the associated ozone production and/or photochemical oxidation may be minimal due to the absorption of UV light by the glass vial.

For the air-exposed samples, the sulfur is oxidized, especially in the air and light exposed sample. The oxidation is seen in the S 2p XPS spectra with a decrease in the bound component and an appearance of a new doublet with S $2p_{3/2}$ component at 166.8–167.1 eV. This is sulfinate, which has been reported to have binding energy of about 166.5 eV [8]. (Alternatively, this same reference reported also seeing sulfonate features at

Table 2
Compositional summary of SAMs relative to a pristine film

Monochrom. Al Kα source	Total S 2p intensity	S 2p oxidized	Presence of O 1s	C 1s intensity	Thickness from Au 4f
Fresh	100%	0%	No	100%	100%
Vial, dark	95 ± 7%	0%	No	98 ± 2%	100 ± 2%
Vial, light	104 ± 7%	3 ± 3%	No	97 ± 2%	98 ± 1%
Air, dark	63 ± 10%	76 ± 6%	Yes	68 ± 2%	76 ± 1%
Air, light	59 ± 10%	97 ± 7%	Yes	59 ± 2%	68 ± 4%
Synchrotron, hv = 280 eV			Presence of oxygen		SAM oriented
Fresh		7 ± 5%	Trace		Yes
Air, light		49 ± 9%	Yes		No

168.4 eV.) Strong changes in the S L-edge spectra and the appearance of O 1s peaks in air-exposed samples strongly support oxidation of the thiolate. Interestingly, the capped samples show only slight oxidation. This lends support to the idea that the process occurs through a dilute atmospheric constituent such as ozone, as reported previously [5,7,9–11]. When the ozone is depleted, the process is quenched, and the remaining gold-bound thiolates survive. One should also note the differences between samples analyzed using XPS only to those investigated with XAS, NEXAFS, and XPS. After exposure, the latter retain more gold-bound thiolates (43%) compared to the former, which may be due to differences (e.g. ozone concentration) at two different locations and two different times. [4]

As the SAMs degrade, various changes occur in the films. The intensity of sulfur and carbon photoemission features correspond to the amount of material on the surface; the reduction in intensity of these two features indicates desorption and a lower concentration of molecules. Au 4f peaks (not shown) increase in intensity. Using the attenuation of the gold photoelectrons in alkanethiolate SAMs [29], this result also indicates fewer molecules reside on the surface in the air-exposed

SAMs compared to the pristine films. Both of these results as well as other compositional results are summarized in Table 2. X-ray absorption further investigates film morphology and chemistry. Similar carbon NEXAFS spectroscopic features exist in both pristine and air-exposed cases. However, a reduction in dichroism indicates a loss of orientational order. Although the polarization dependence is less pronounced, these spectra indicate molecules are statistically more upright than prostrate. Considering the measured mixture of oxidized and thiolate sulfur species in this case, these results could be due to a mixed phase where intact molecules are at a polar angle similar to undisturbed SAMs, while molecules with sulfinate bases are flat on the surface as seen in previous STM measurements on oxidized SAM molecules [13]. R*/C–H σ* features are attenuated due to the chemical and structural changes occurring in the molecules. Finally, shifts in energy and peak broadening in the C 1s peaks with air exposure are consistent with both changes toward a less ordered monolayer [30] and changes in carbon chemical environments.

5. Conclusions

X-ray photoelectron spectra of S 2p, C 1s, and O 1s core-levels have been measured for dodecanethiol-based self-assembled monolayers on Au(1 1 1), both freshly prepared, and exposed to various levels of ambient laboratory conditions. Samples were removed from solutions, rinsed in ethanol, and placed in dark capped vials, capped

---

[4] Ozone concentration in vicinity of two locations varies. For May 16–17, 2002 in Livermore, CA, USA (five XPS samples) ozone at a nearby monitoring station was 28 ppb (52 peak) and 30 ppb (42 peak); while for Redwood City, CA, near SSRL @ SLAC, ozone registered 18 ppb (27 ppb max) and 18 ppb (28 ppb max) for July 5–6, 2002, dates of exposure and analysis. Source: Bay Area Air Quality Management District, http://www.baaqmd.gov.

vials under light, and under air exposure in uncapped vials in both darkness and light. Capped vial samples survive reasonably well, retaining sulfur–gold bonds and losing only a few percent of the molecules. SAMs stored in uncapped vials, exposed to air, degrade rapidly. Sulfur features oxidize, as seen in chemical shifts of S 2p and the appearance of O 1s photoelectrons.

The sulfur L-edge X-ray absorption spectra, and carbon K-edge NEXAFS have also been measured. Sulfur absorption spectra change upon exposure to air, consistent with XPS results indicating oxidation. Freshly prepared samples have the expected high polarization dependence in carbon NEXAFS, indicative of well-packed, ordered films. SAMs which have been exposed to air have some polarization dependence, but much less than fresh SAMs indicating the layer has significantly less orientational order.

These results have important implications for applications that depend upon the durability of SAMs under atmospheric conditions. Although ease of preparation and stability of alkanethiols adsorbed on gold are thus far unmatched by any other method or system for SAM formation, the often-made assumption that the gold thiolate bond is ultra-robust and stable under ambient conditions is false. Alkanethiols, or other organics adsorbed on gold through gold–thiolate bonding degrade rapidly when exposed to air. Care must be taken to avoid SAM degradation by using freshly prepared samples, carefully storing samples in benign environments, and quantitatively characterizing films to ensure alkanethiolates on gold have sufficient durability for each intended application.

References

[1] N.T. Flynn, T.N.T. Tran, M.J. Cima, R. Langer, Langmuir 19 (2003) 10909.
[2] Y.Z. Li, J.Y. Huang, R.T. Mciver, J.C. Hemminger, Journal of the American Chemical Society 114 (1992) 2428.
[3] J.R. Scott, L.S. Baker, W.R. Everett et al., Analytical Chemistry 69 (1997) 2636.
[4] M.J. Tarlov, J.G. Newman, Langmuir 8 (1992) 1398.
[5] C.G. Worley, R.W. Linton, Journal of Vacuum Science and Technology A—Vacuum Surfaces and Films 13 (1995) 2281.
[6] N.J. Brewer, R.E. Rawsterne, S. Kothari, G.J. Leggett, Journal of the American Chemical Society 123 (2001) 4089.
[7] M.H. Schoenfisch, J.E. Pemberton, Journal of the American Chemical Society 120 (1998) 4502.
[8] M.T. Lee, C.C. Hsueh, M.S. Freund, G.S. Ferguson, Langmuir 14 (1998) 6419.
[9] K.L. Norrod, K.L. Rowlen, Journal of the American Chemical Society 120 (1998) 2656.
[10] Y.M. Zhang, R.H. Terrill, T.A. Tanzer, P.W. Bohn, Journal of the American Chemical Society 120 (1998) 2654.
[11] Y. Zhang, R.H. Terrill, P.W. Bohn, Chemistry of Materials 11 (1999) 2191.
[12] G.E. Poirier, E.D. Pylant, Science 272 (1996) 1145.
[13] G.E. Poirier, T.M. Herne, C.C. Miller, M.J. Tarlov, Journal of the American Chemical Society 121 (1999) 9703.
[14] A.L. Vance, T.M. Willey, A.J. Nelson, T. van Buuren, C. Bostedt, L.J. Terminello, G.A. Fox, Langmuir 18 (2002) 8123.
[15] A.L. Vance, T.M. Willey, T. van Buuren, A.J. Nelson, C. Bostedt, G.A. Fox, L.J. Terminello, Nano Letters 3 (1) (2003) 81.
[16] N. Weber, C. Hamann, J.-M. Kern, J.-P. Sauvage, Inorganic Chemistry 42 (2003) 6780.
[17] T. Lu, L. Zhang, G.W. Gokel, A.E. Kaifer, Journal of the American Chemical Society 115 (1993) 2542.
[18] G.K. Tirsell, V.P. Karpenko, Nuclear Instruments and Methods in Physics Research A291 (1990) 511.
[19] T.M. Willey, A.L. Vance, T. van Buuren, C. Bostedt, A.J. Nelson, L.J. Terminello, C.S. Fadley, Langmuir 20 (2004) 2746.
[20] J. Stöhr, NEXAFS Spectroscopy, Springer Verlag, Berlin Heidelberg, 1992.
[21] J. Stöhr, D.A. Outka, Physical Review B 36 (15) (1987) 7891.
[22] A.P. Hitchcock, J. Stöhr, J.A. Horsley, R.D. Redwing, A. Johnson, F. Sette, Journal of Chemical Physics 85 (9) (1986) 4849.
[23] P. Bagus, K. Weiss, A. Schertel, C. Wöll, W. Braun, C. Hellwig, C. Jung, Chemical Physics Letters 248 (1996) 129.
[24] D.G. Castner, K. Hinds, D.W. Grainger, Langmuir 12 (1996) 5083.

[25] M. Zharnikov, S. Frey, K. Heister, M. Grunze, Langmuir 16 (2000) 2697.

[26] K. Heister, M. Zharnikov, G.M.L.S. Johansson, A. Ullman, Langmuir 17 (2001) 8.

[27] M. Zharnikov, M. Grunze, Journal of Vacuum Science and Technology B 20 (5) (2002) 1793.

[28] J. Thome, M. Himmelhaus, M. Zharnikov, M. Grunze, Langmuir 14 (1998) 7435.

[29] C.L.A. Lamont, J. Wilkes, Langmuir 15 (6) (1999) 2037.

[30] K. Heister, L.S. Johansson, M. Grunze, M. Zharnikov, Surface Science 529 (2003) 36.